
Emergent mechanisms for long timescales depend on training curriculum and affect performance in memory tasks

Sina Khajehabdollahi^{1,2,*}, Roxana Zeraati^{1,3,*}, Emmanouil Giannakakis^{1,3},
Tim Jakob Schäfer^{1,3}, Georg Martius^{1,2}, Anna Levina^{1,3,4}

¹ University of Tübingen, Germany

² Max Planck Institute for Intelligent Systems, Tübingen, Germany

³ Max Planck Institute for Biological Cybernetics, Tübingen, Germany

⁴ Bernstein Network Computational Neuroscience Tübingen

* These authors contributed equally to this work.

Abstract

Recurrent neural networks (RNNs) in the brain and *in silico* excel at solving tasks with intricate temporal dependencies. Long timescales required for solving such tasks can arise from properties of individual neurons (single-neuron timescale, τ , e.g., membrane time constant in biological neurons) or recurrent interactions among them (network-mediated timescale, τ_{net}). However, the contribution of each mechanism for optimally solving memory-dependent tasks remains poorly understood. Here, we train RNNs to solve N -parity and N -delayed match-to-sample tasks with increasing memory requirements controlled by N by simultaneously optimizing recurrent weights and τ s. We find that for both tasks RNNs develop longer timescales with increasing N , but depending on the learning objective, they use different mechanisms. Two distinct curricula define learning objectives: sequential learning of a single- N (single-head) or simultaneous learning of multiple N s (multi-head). Single-head networks increase their τ with N and are able to solve tasks for large N , but they suffer from catastrophic forgetting. However, multi-head networks, which are explicitly required to hold multiple concurrent memories, keep τ constant and develop longer timescales through recurrent connectivity. Moreover, we show that the multi-head curriculum increases training speed and network stability to ablations and perturbations, and allows RNNs to generalize better to tasks beyond their training regime. This curriculum also significantly improves training GRUs and LSTMs for large- N tasks. Our results suggest that adapting timescales to task requirements via recurrent interactions allows learning more complex objectives and improves the RNN's performance.

1 Introduction

The interaction of living organisms with their natural environment requires the concurrent processing of signals over a wide range of timescales, from perceiving sensory stimuli on a scale of milliseconds [1] to the much longer timescales of more complex processes such as working memory [2]. The diverse timescales of these tasks are reflected in the dynamics of the neural populations that perform the corresponding computations in biological neural networks [3, 4, 5, 6] by scaling their timescales according to task requirements [5, 7]. At the same time, artificial neural networks performing memory-demanding tasks (speech [8], handwriting [9], sketch [10], language recognition/synthesis [11], time-series prediction [12, 13], music composition [14]) need to process the long temporal dependency of sequential data over variable timescales. Recurrent neural networks (RNNs) [15, 16, 17, 18]

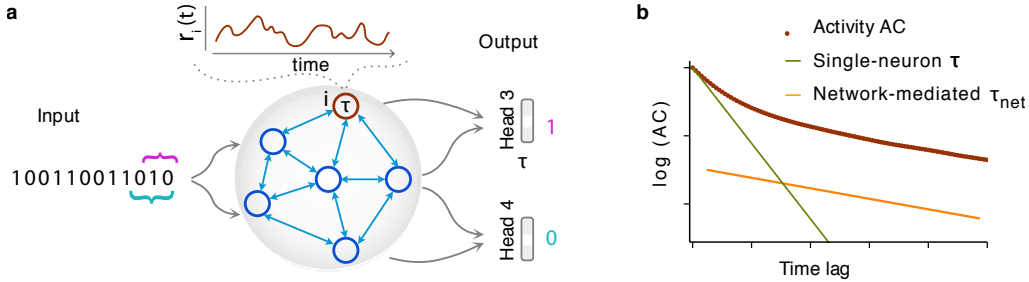


Figure 1: Schematics of network structure and timescales. **a.** An outline of the network. A binary sequence is given as input to a leaky RNN, with each neuron’s intrinsic timescale being a trainable parameter τ . The illustration shows the N -parity task with readout heads for $N = 3$ and $N = 4$. **b.** An illustration of the manifestation of different timescales (single-neuron and network-mediated) on the autocorrelation of a network neuron (see also Fig. S10).

have been introduced as a machine learning tool that can learn such temporal dependencies using back-propagation through time.

In biological neural networks, the emergence of diverse neural timescales occurs via a variety of interacting mechanisms. The timescales of individual neurons’ activity are determined by cellular and synaptic processes, such as the membrane or synaptic time constants that vary across brain areas and neuron types [19, 20]. These single-neuron timescales characterize the timescale of neural activity in the absence of recurrent interactions. However, neurons are embedded within rich network structures that also shape neural dynamics introducing network-mediated timescales. The strength of recurrent connections [21, 22, 23], as well as their topology [24, 25, 7, 26] give rise to network-mediated timescales that can be much longer than single-neuron timescales.

Heterogeneous and tunable single-neuron timescales have been proposed as a mechanism to adapt the timescales of RNN dynamics to task requirements and improve their performance [27, 28, 29, 30, 31, 32]. In these studies, the time constants of individual neurons are trained together with network connectivity. For tasks with long temporal dependencies, the distribution of trained single-neuron timescales becomes heterogeneous according to the task’s memory requirements [27]. Explicit training of single-neuron timescales improves network performance in benchmark RNN tasks in rate [28, 29] and spiking [30, 31, 27] networks and leads to greater robustness [27] and adaptability to novel stimuli [32]. While these studies propose the adaptability of single-neuron timescales as a potential mechanism for solving time-dependent tasks, the exact contribution of single-neuron and network-mediated timescales in optimally solving the tasks is unknown.

Here, we study how single-neuron and network-mediated timescales shape the dynamics and performance of RNNs trained on long-memory tasks. We show that the extent to which longer single-neuron or network-mediated timescales are necessary for solving such tasks largely depends on the learning objective (as defined by different curricula). Challenging the common beliefs in the field, we identify settings where trainable single-neuron timescales offer no advantage in solving temporal tasks. We demonstrate that adapting RNNs’ timescales using network-mediated mechanisms instead of single-neuron timescales increases training speed and network stability to perturbations and enables RNNs to generalize better to tasks beyond their training regime.

2 Model

We approximate the effect of the membrane timescale of biological neurons by equipping each RNN-neuron with a trainable leak parameter τ , which defines the timescale of the individual neurons, independent of network interactions (Fig. 1a). Each leaky-RNN contains 500 neurons, and the activity of each neuron evolves over discrete time steps t governed by:

$$r_i(t) = \left[\left(1 - \frac{1}{\tau_i} \right) \cdot r_i(t-1) + \frac{1}{\tau_i} \cdot \left(\sum_{j \neq i} W_{ij}^R \cdot r_j(t-1) + W_i^I \cdot S(t) + b^R + b^I \right) \right]_{\alpha}, \quad (1)$$

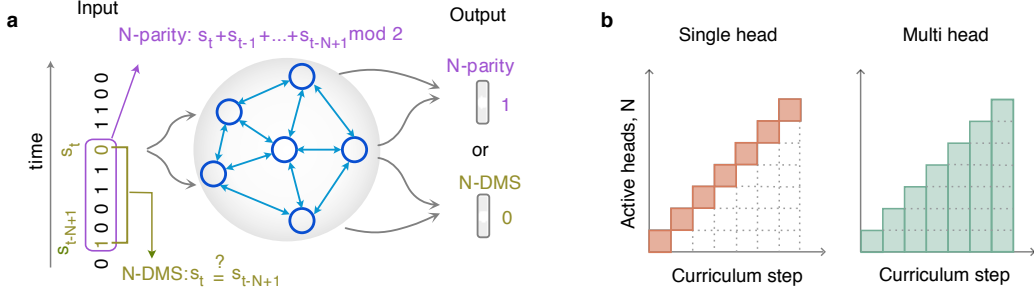


Figure 2: Schematic description of the tasks and curricula **a**. An outline of the network and tasks. In both tasks, the network receives a binary input sequence, one bit at each time step. **b**. In the single-head curriculum, only one read-out head is trained at each curriculum step, while in the multi-head curriculum, a new read-out head is added at each step without removing the older heads.

where $[\cdot]_\alpha$ is the leaky ReLU function with negative slope α , given by:

$$[x]_\alpha = \begin{cases} x, & x \geq 0 \\ \alpha \cdot x, & x < 0. \end{cases} \quad (2)$$

For all networks, we use $\alpha = 0.1$. We obtain similar results using a different type or location of non-linearity (Appendix A). W^R, b^R and W^I, b^I are the recurrent and input weights and biases respectively, S is the binary input given to the network at each time step, and $\tau_i \geq 1$ is the trainable timescale of the neuron. The network receives uncorrelated binary inputs updated every k time steps. Unless stated otherwise, we consider $k = 1$. When $\tau = 1$, the neurons become memory-less (i.e., the state of the neuron at time t only depends on the input it receives at that point and not on its activity at time $t - 1$). In contrast, for $\tau > 1$, the neuron’s activity depends on its activity at the previous time steps, and the dependence increases with τ . In the limit case $\tau \rightarrow \infty$, the neuron’s activity is constant, and the input has no effect.

The dynamics of each neuron can be characterized by two distinct timescales: (i) single neuron timescale τ , (ii) network mediated timescale τ_{net} . The single neuron timescale τ gives the intrinsic timescale of a neuron in the absence of any network interaction, while the network-mediated timescale τ_{net} emerges through the learned connectivity and represents the effective timescale of the neuron’s activity as part of the network. For networks with linear dynamics, τ_{net} can be directly estimated from the eigenvalues of the connectivity matrix [25]. However, using this method is not possible for our networks due to the non-linear dynamics. Instead, τ_{net} can be effectively estimated from the decay rate of the autocorrelation function. The autocorrelation of a neuron’s activity, defined by Eq. 1, can be approximated by two distinct timescales which appear as two slopes in logarithmic-linear coordinates (Fig. 1b) [26]. The steep initial slope indicates the single-neuron timescale (τ), and the shallower slope indicates the network-mediated timescale (τ_{net}). It has been shown analytically that in RNNs, τ_{net} depends on τ and the network structure [26]. Hence, τ_{net} can be modulated by τ and depending on the structure of the network $\tau_{\text{net}} \leq \tau$ [26].

We estimate the network-mediated timescales from the autocorrelation of each neuron’s activity, while the network is driven by uncorrelated binary input sampled at each time step from a Bernoulli distribution. To avoid autocorrelation bias in our estimations [6], we simulate network activity for long periods ($T = 10^5$ time steps). We compute the autocorrelation of each neuron i at time-lag t' as

$$\text{AC}_i(t') = \frac{1}{\hat{\sigma}_i^2(T - t')} \sum_{t=0}^{T-t'} (r(t) - \hat{\mu}_i)(r(t - t') - \hat{\mu}_i), \quad (3)$$

where $\hat{\mu}_i$ and $\hat{\sigma}_i^2$ are the sample mean and sample variance of neuron’s i activity, respectively. We simulated each network for 10 trials (i.e. 10 distinct realizations of inputs with duration $T = 10^5$) and computed the average autocorrelation of each neuron across trials. To estimate τ_{net} , we fit the average autocorrelation once with a single- ($\tau_{\text{net}} = \tau$) and once with a double-exponential ($\tau_{\text{net}} > \tau$) decay function using the non-linear least-squares method. Then, we determine the corresponding timescales for both models and use the Akaike Information Criterion (AIC) [33] to select the best-fitting model. When the double-exponential model is selected, the slowest of the two timescales indicates τ_{net} . For

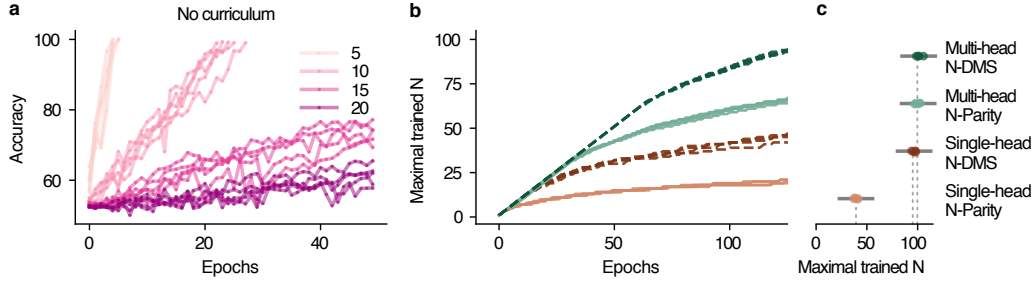


Figure 3: Training performance depends on the curriculum. **a.** Training the networks without a curriculum leads to stagnated learning when N is large. For each N , 5 models are independently trained for 50 epochs or until the task is solved ($> 98\%$ accuracy). **b.** When training with a curriculum, the networks are better at solving larger N s within the same training time. **c.** The maximum trained N for each type of task/curriculum at the end of training (1000 epochs, 3 days, or solving $N = 101$, whichever comes first). Gray lines - mean value across 4 trained networks.

most fits, we obtain a large coefficient of determination, confirming that the two selected functions capture well the autocorrelation shapes (Fig. S10).

3 Setup

3.1 Tasks

In both tasks, a binary sequence s of length $L > N$ is given as the input, one bit at each time step. We train the networks on sequences with lengths uniformly chosen from the interval $L \in \{N + 2, 4N\}$.

N -parity: The network has to output the binary sum (XOR) of the last N digits, indicating an odd or even number of non-zero digits. To solve the task, the network needs to store the values and order of the last N digits in memory, since at each time step, the value of the digit presented to the network at t needs to be added, and the value of the digit presented at $t - N$ needs to be subtracted from the running sum (Fig. 2a).

N -delayed match-to-sample (N -DMS): The network has to output 1 or 0 to indicate whether the digit presented at current time t matches the digit presented at time $t - N + 1$. The memory requirement for this task is similar to N -parity, since the value of all digits presented between time t and $t - N + 1$ need to be stored in memory (Fig. 2a).

3.2 Training

We train the single-neuron timescales $\tau = \{\tau_1, \dots, \tau_{500}\}$, the weights and biases W^R, b^R and W^I, b^I , and a linear readout layer via back-propagation through time using a stochastic gradient descent optimizer with Nesterov momentum and a cross-entropy loss. Each network is trained on a single Nvidia GeForce 2080ti for a maximum of 1000 epochs, 3 days, or until the $N = 101$ task is solved, whichever comes first. RNNs are trained without any regularization. Including L2 regularization achieves comparable performance.

Single-head training: Starting with $N = 2$, we train the network to reach an accuracy of 98%. We then use the trained network parameters to initialize the next network that we train for $N + 1$ (Fig. 2b).

Multi-head training: As with the single-head networks, we begin with a network solving a task for $N = 2$, but now, once a threshold accuracy of 98% is reached, a new readout head is added for solving the same task for $N + 1$, preserving the original readout heads. At each curriculum step, all readout heads are trained simultaneously (the loss is the sum of all readout heads' losses) so that the network does not forget how to solve the task for smaller N s (Fig. 2b).

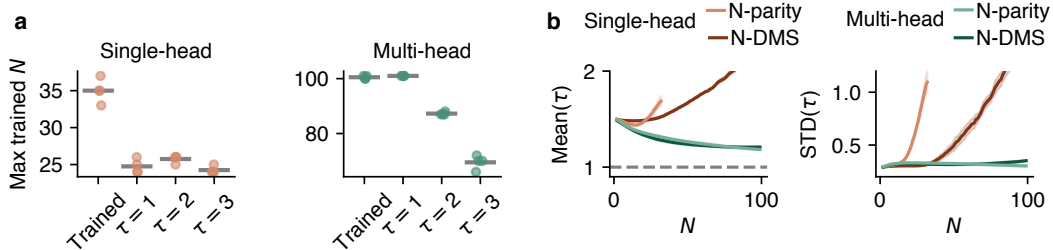


Figure 4: Importance of single-neuron timescales for different curricula. **a.** The maximum N solved in the N -bit parity task after 1000 epochs (reaching an accuracy of 98%). In the single-head curriculum, models rely on training τ , whereas in the multi-head curriculum, having τ s fixed at k value is as good as training them. Horizontal bars - mean. **b.** The mean and standard deviation (STD) of the trained τ s increase with N in single-head networks. In contrast, in multi-head networks, the mean τ decreases towards $k = 1$, and the STD remains largely constant. The mean and STD are computed across neurons within each network (up to the maximum N shared between all trained networks). Shading - variability across 4 trained networks.

4 Results

Here, we present an analysis of the dynamics and performance of trained RNNs across tasks and training curricula. Our investigation aims to shed light on the factors influencing network performance and robustness. First, we explore which conditions improve network performance, i.e., allow solving tasks for larger N . To uncover the mechanisms that lead to differences in performance, we study how single-neuron and network-mediated timescales change relative to task difficulty. Finally, we ask which trained networks are more robust to various perturbations. This multifaceted approach aims to enhance our understanding of the interaction between training mechanisms, network dynamics, and the resulting performance and robustness.

4.1 Performance under different curricula

Our objective is to learn the largest possible N in each task. First, we test whether good task performance can be achieved for high N in either of our tasks without using a curriculum. We find that for both tasks, the networks struggle to reach high accuracy for $N > 10$ (Fig. 3a) when trained directly. On the other hand, using either curriculum significantly boosts the network’s capacity to learn both tasks for much higher N , (Fig. 3b).

Despite improved performance using any of the two curricula, task performance differs significantly between them. The single-head networks can reliably reach $N \approx 35$ for the N -parity and $N \approx 90$ for the N -DMS task. The difference in performance between the two tasks is expected because the N -DMS task is much easier than the N -parity task. However, the multi-head networks can reliably reach $N \geq 100$ for both tasks and require fewer training epochs to reach %98 accuracy for each N (Fig. 3b, c). Networks that are trained using an intermediate curriculum between the two extremes of single- and multi-head (i.e., solving simultaneously $H < N$ tasks for $N, N - 1, \dots, N - H + 1$ with gradually shifting N s) exhibit an intermediate performance (Appendix B). Overall, the multi-head networks outperform the single-head ones in terms of performance (maximum N reached) and the required training time. Moreover, the multi-head curriculum significantly improves the training of other recurrent architectures such as GRU and LSTM to perform large- N tasks (Appendix C), suggesting that the multi-objective curriculum can generally improve learning long-memory tasks.

The superior performance of the multi-head networks may be counter-intuitive given that they are required to solve the task for every $N \leq m$ at the m -th step of the curriculum, whereas the single-head networks are only required to solve it for exactly $N = m$. However, we find that the single-head networks suffer from catastrophic forgetting: a network trained for higher N cannot perform the task for lower N s it was trained for during the curriculum, even after retraining the readout weights. These results suggest that explicit prevention of catastrophic forgetting by learning auxiliary tasks (i.e. tasks with N smaller than objective, $N < m$) facilitates learning high N s. Furthermore, the multi-head curriculum emerges when training on a multi-objective task without introducing an explicit curriculum (Appendix D), supporting the optimal strategy of this curriculum.

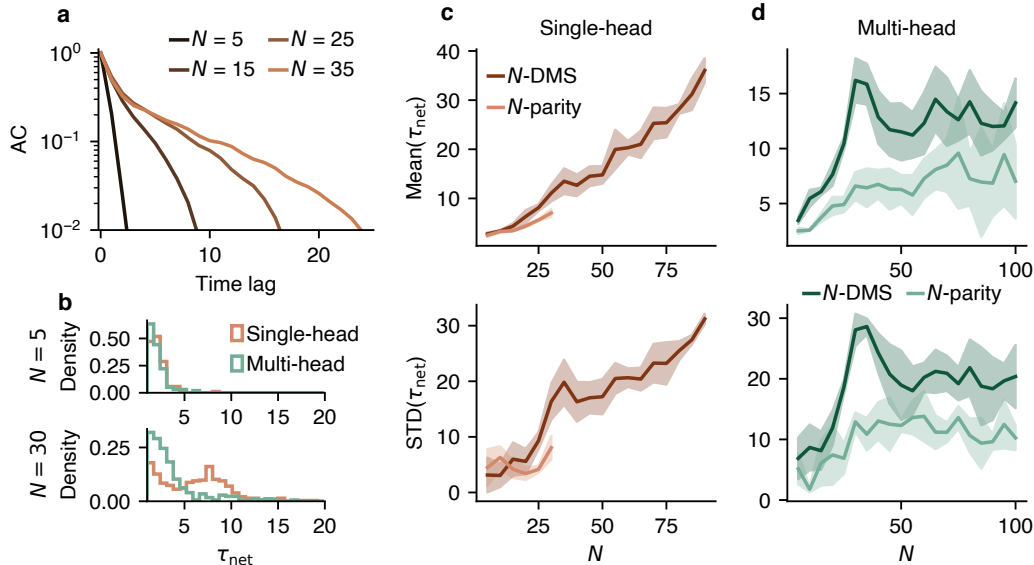


Figure 5: The emergence of network-mediated timescales depends on the curriculum. **a.** Example average autocorrelations of all the neurons within a network. The autocorrelations of individual neurons’ activity decay slower with increasing N . **b.** Distributions of the network-mediated timescales τ_{net} for single and multi-head networks solving N -parity task for $N = 5$ and $N = 30$. The distribution becomes broader for higher N . **c, d.** The mean and STD of the network-mediated timescale τ_{net} increase with N in both tasks. The mean and STD are computed across neurons within each network. Shades - variability across 4 trained networks.

We additionally examine the impact of training single-neuron timescales on training performance. To this end, we compare the training performance of networks with a fixed $\tau \in \{1, 2, 3\}$ shared across all neurons versus networks with trainable timescales. In the single-head curriculum, the training performance with fixed τ is significantly worse than when we train τ (Fig. 4a). On the other hand, the multi-head networks perform equally well in the case where we fix $\tau = 1$ (i.e., $\tau = k$) and in the case where the τ is trained, but the performance steeply declines for fixed $\tau \geq 2$ (Fig. 4b). These results indicate that single-head networks rely on single-neuron timescales for solving the task, whereas multi-head networks only use τ to track the timescale of updating the input k and use other mechanisms to hold the memory, which we discuss in the following.

4.2 Mechanisms underlying long timescales

To understand the mechanisms underlying the difference in the performance of networks trained under single and multi-head curricula, we study how single-neuron and network-mediated timescales change with increasing task difficulty. One can expect that as the timescale of the task (mediated by N) increases, neurons would develop longer timescales to integrate the relevant information. Such long timescales can arise either by directly modulating τ for each neuron or through recurrent interactions between neurons reflected in τ_{net} . Thus, we investigate how τ and τ_{net} change with N as each curriculum progresses.

The two curricula adjust their single-neuron timescales to N in distinct ways (Fig. 4b). For the single-head curriculum, the mean and variance of τ increase with N , suggesting that not only do single-neuron timescales become longer as the memory requirement grows, but they also become more heterogeneous. We obtain similar results for networks trained without curricula (Fig. S11). These results align with previous findings that the heterogeneity of single-neuron timescales improves networks’ performance in temporal tasks [27]. On the contrary, we find that in multi-head networks, the average τ decreases with N , approaching $k = 1$ as the curriculum progresses. Similar results can be obtained when $k > 1$ (i.e. $\tau \rightarrow k$, Appendix E). The trend of $\tau \rightarrow 1$ for high N is consistent with the fact that the multi-head networks with fixed $\tau = 1$ performed as well as the networks with trained

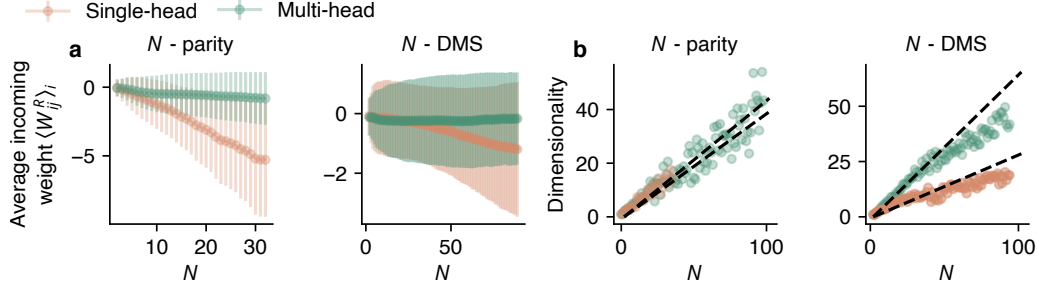


Figure 6: Learned recurrent connectivity and dimensionality of population activity. **a.** The average incoming weight to a neuron remains close to zero for multi-head networks but becomes strongly negative as N increases in single-head networks (example RNN). Error bars - \pm STD. **b.** The dimensionality of the activity increases linearly with N in N -parity and sub-linearly in N -DMS task. Dashed lines - regression lines computed up to $N = 30$, approximating potential linear relations.

τ . Consequently, in these networks, the memory of each neuron only depends on the previous state of other neurons and not on its past state.

Network-mediated timescales generally increase with N in both curricula (Fig. 5). The increase of τ_{net} can be observed in the autocorrelation of individual neurons, as they decay slower with increasing N (Fig. 5a). In networks trained for higher N s, neurons with slower τ_{net} emerge and τ_{net} s become more heterogeneous (Fig. 5b). In single-head networks, the mean and variance of τ_{net} follow a similar trend as τ (Fig. 5c). This result is expected analytically [26] since the increase in τ would increase τ_{net} . The mean and variance of τ_{net} in multi-head networks increase with N up to some intermediate N , but the pace of increase reduces gradually and saturates for very large N s (Fig. 5d, top). Given the small single-neuron timescales in these multi-head networks, the long τ_{net} s and their heterogeneity can only arise from recurrent interactions between neurons that are shaped by the structure of network connectivity and population dynamics.

We next examine if there are any observable differences between the recurrent connectivity patterns and population dynamics of the two network types (Fig. 6). We find the multi-head networks have, on average, almost the same total incoming positive and negative weights (with a slight tendency towards the larger total negative weights as N increases), leading to relatively balanced dynamics (Fig. 6a). On the other hand, single-head networks are much less balanced, with a strong bias towards more inhibition (negative weights) as N increases. The strong negative weights in single-head networks are required to create stable dynamics in the presence of long single-neuron timescales. At the same time, the dimensionality of population activity (measured as the number of principal components that explain 90% of the variance) increases almost linearly with N in the N -parity task but sub-linearly in the N -DMS task, using both curricula, reflecting distinct computational requirements for solving the two tasks (Fig. 6b).

Our findings suggest that while there is a common pattern of network activity (high-dimensional activity with long autocorrelations/ τ_{net}), the two curricula generate this activity with distinct mechanisms. The single-head networks develop slow single-neuron timescales τ that increase with N , combined with strong inhibitory recurrent connectivity. In contrast, the multi-head networks maintain relatively balanced connectivity and push the single-neuron timescales close to k . The significant difference in performance suggests that the second mechanism is more effective in solving the task.

4.3 Implications of different curricula for network performance

To compare the robustness and re-training capability between the two curricula, we investigate changes in network accuracy resulting from ablations, perturbations, and re-training networks on unseen N . We measure the effects on network performance using a relative accuracy metric with respect to the originally trained network, defined as $\text{acc}_{\text{rel}} := (\text{acc} - 0.5) / (\text{acc}_{\text{base}} - 0.5)$, where acc_{base} represents the accuracy of the network before any perturbations or ablations, acc is the measured accuracy after the intervention, and 0.5 is a chance level used for the normalization. If $\text{acc}_{\text{rel}} = 1$, the intervention did not change the accuracy; when $\text{acc}_{\text{rel}} \approx 0$, the intervention reduced the accuracy to random guessing. All accuracies are evaluated only on the maximal trained N .

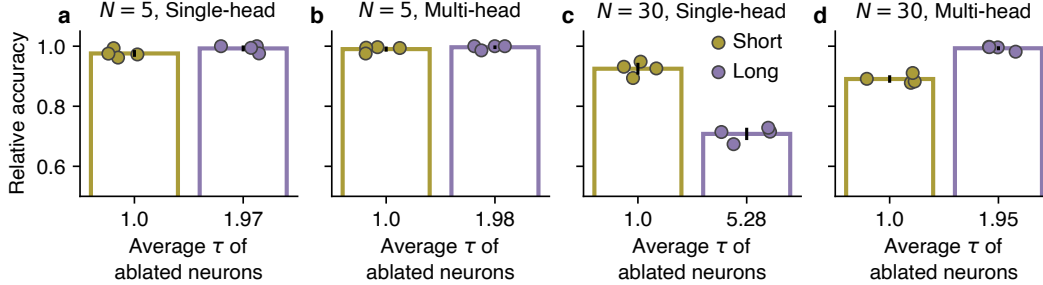


Figure 7: Impact of ablating neurons with distinct timescales on RNNs’ performance. **a, b.** Ablating the longest and shortest timescale neurons has minimal effect on network performance when N is small for both curricula. **c, d.** For higher N , ablating long-timescale neurons largely decreases the performance of single-head networks, while multi-head networks are more affected by the ablation of short-timescale neurons. Bars - mean, error bars - STD, dots - 4 individual networks.

Ablation: To examine the relative impact of neurons with different trained timescales τ on network performance, we ablate individual neurons based on their τ and measure network performance without re-training. Specifically, we compare the effect of ablating the 20 longest (4% of the network) and 20 shortest timescale neurons from the network (Fig. 7). When N is small, for both curricula, ablating individual neurons has only minimal effect on accuracy (Fig. 7a,b). However, for larger N , we observe a considerable difference in the importance of neurons. Single-head networks rely strongly on long-timescale neurons (Fig. 7c), such that ablating them reduces the performance much more than for short-timescale neurons. In contrast, multi-head networks exhibit greater robustness against ablation, and their accuracy is more affected when short-timescale neurons (i.e., neurons with $\tau = k$) are ablated (Fig. 7d). Note that in the single-head network, the average of the 20 longest single-neuron timescales is 2.7 times longer than in the multi-head network.

Perturbation: We investigate the perturbation of recurrent weights W^R and timescales τ with strength ε . The perturbed weights and timescales are computed as

$$\widetilde{W}^R = W^R + \varepsilon \frac{\xi_W}{\|\xi_W\|} \|W^R\|, \quad \widetilde{\tau} = \tau + \varepsilon \left| \frac{\xi_\tau}{\|\xi_\tau\|} \|\tau\| \right|, \quad (4)$$

where $\xi_W \sim \mathcal{N}(0, \mathbb{I}^{n \times n})$, and $\xi_\tau \sim \mathcal{N}(0, \mathbb{I}^n)$. $\|\cdot\|$ represents the Frobenius norm and $|\cdot|$ denotes the absolute value. This perturbation scheme is inspired by adversarial studies [34]. τ is perturbed positively to avoid $\tau < 1$.

Multi-head networks are more robust to perturbations of recurrent weights (Fig. 8a) and timescales (Fig. 8b). The robustness of multi-head networks to perturbations in recurrent weights is particularly noteworthy since these networks rely on connectivity to mediate long timescales. This observation indicates that the overall robustness extends to network connectivity as well.

Re-training: We evaluate the performance of networks that solve $N = 16$, when re-trained without curriculum (without training on intermediate N s) for an arbitrary higher N , after 20 epochs. Multi-head networks show a superior re-training ability compared to single-head networks for at least 10 N beyond $N = 16$ (Fig. 8c). This finding suggests that multi-head networks are better at learning the underlying task and adjust faster to a new, larger N even when skipping intermediate N s.

5 Related Work

The question of how task-dependent timescales arise in neural networks and their implications for performance and robustness has been the subject of extensive research. Several studies have examined how functional timescales emerge from training the connectivity of a recurrent network to perform specific tasks. Specifically, it has been shown that balanced connectivity [35], strong inhibition [36] or homeostatic plasticity [37, 38] can lead to the development of long timescales in networks solving memory tasks. Additionally, different studies have explored how the explicit inclusion of trainable timescales in a model can improve performance in spiking networks [27, 36] as well as in recurrent architectures such as LSTMs [39, 40]. Moreover, LSTM performance improves significantly when equipped with multiple timescales [41, 39, 42].

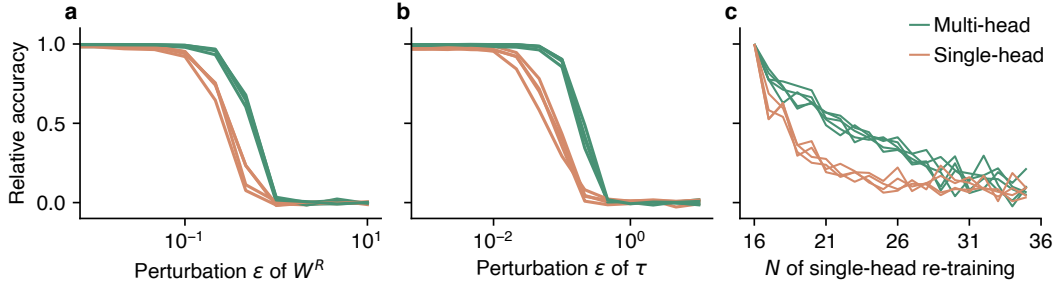


Figure 8: Robustness to perturbation and re-training performance depends on curriculum. **a, b.** Multi-head networks are more robust against perturbations of recurrent connectivity (a) and trained timescale τ (b) than single-head networks. **c.** Networks trained to solve $N = 16$ re-trained to solve a higher N without curriculum (relative accuracy after 20 epochs). Multi-head networks achieve a higher relative accuracy when re-trained for 20 epochs in comparison to single-head networks. Lines - individual networks. Shades - \pm STD (4 networks for each curriculum).

In this study, we relate the mechanisms of task-dependent timescale emergence with the learning dynamics of RNNs and particularly the use of specific curriculum learning protocols. Curriculum learning has been proposed as a fitness landscape-smoothing mechanism that can enable the gradual learning of highly complex tasks [43, 44, 45]. It has been shown that choosing different curricula can lead to distinct learning outcomes in networks training for the same task [46]. Here, we extend these findings by demonstrating how different curricula can push networks towards adopting different strategies for developing the necessary dynamics for solving long-memory tasks.

6 Conclusion

We find that to solve temporal tasks with varying memory requirements, RNNs develop high-dimensional activity with slow timescales. We identify two distinct combinations of connectivity and single-neuron timescales that generate this beneficial activity, each produced via a different curriculum. While the single-head curriculum crucially relies on the long single-neuron timescales to generate long network timescales, the multi-head network prefers single-neuron timescales to be constant and solves the task relying only on the long timescales emerging from recurrent interactions. Finally, we show that the multi-head curriculum leads not only to better performance but also to greater robustness to a variety of perturbations and a greater ability to generalize.

Our findings suggest that training networks on *sets* of related tasks instead of a single task leads to networks that train faster, reach higher performance, and are more robust to perturbations. By progressively shaping the loss function of our network with a curriculum to include performance evaluations on sub-tasks that are known to correlate with the desired task, we can smooth the loss landscape of our network to allow training for difficult tasks that were previously unsolvable without a curriculum. In this way, choosing an appropriate curriculum can act as a powerful regularization.

Finally, our results indicate that while relatively long timescales are a ubiquitous requirement for solving temporal tasks, they do not have to originate from the slow timescales of individual neurons and can be effectively created by connectivity. Moreover, trainable single-neuron timescales are not necessarily advantageous for learning long memory tasks and depend on the task’s objective. For learning more complex objectives (e.g., holding multiple memories at the same time), using network-mediated timescales gives more stable solutions. The choice of training curriculum can push the network into the appropriate dynamical regime without explicitly training single-neuron timescales. Indeed, we find that very fast single-neuron timescales (in the case of the multi-head network) do not preclude the development of slow network-mediate timescales and can even lead to improved network performance.

Limitations: Our study considers only two relatively simple tasks but with explicitly controllable memory requirements. It would be interesting to test our observations in real-world tasks and investigate whether our results apply to other architectures and optimizers.

Acknowledgments

This work was supported by a Sofja Kovalevskaja Award from the Alexander von Humboldt Foundation, endowed by the Federal Ministry of Education and Research (SK, RZ, EG, AL) and Else Kröner Medical Scientist Kolleg "ClinbrAI: Artificial Intelligence for Clinical Brain Research" (TJS). AL and GM are members of the Machine Learning Cluster of Excellence, EXC number 2064/1 – PN 390727645. We acknowledge the support from the BMBF through the Tübingen AI Center (FKZ: 01IS18039B), International Max Planck Research School for the Mechanisms of Mental Function and Dysfunction (IMPRS-MMFD) and International Max Planck Research School for Intelligent Systems (IMPRS-IS). We thank Victor Buendía for valuable discussions.

References

- [1] Brice Bathellier, Derek L. Buhl, Riccardo Accolla, and Alan Carleton. Dynamic ensemble odor coding in the mammalian olfactory bulb: Sensory information at different timescales. *Neuron*, 57(4):586–598, 2008.
- [2] John Jonides, Richard L. Lewis, Derek Evan Nee, Cindy A. Lustig, Marc G. Berman, and Katherine Sledge Moore. The Mind and Brain of Short-Term Memory. *Annual Review of Psychology*, 59(1):193–224, 2008.
- [3] John D. Murray, Alberto Bernacchia, David J. Freedman, Ranulfo Romo, Jonathan D. Wallis, Xinying Cai, Camillo Padoa-Schioppa, Tatiana Pasternak, Hyojung Seo, Daeyeol Lee, and Xiao-Jing Wang. A hierarchy of intrinsic timescales across primate cortex. *Nature Neuroscience*, 17(12):1661–1663, December 2014.
- [4] Sean E. Cavanagh, Laurence T. Hunt, and Steven W. Kennerley. A Diversity of Intrinsic Timescales Underlie Neural Computations. *Frontiers in Neural Circuits*, 14, 2020. Publisher: Frontiers.
- [5] Richard Gao, Ruud L van den Brink, Thomas Pfeffer, and Bradley Voytek. Neuronal timescales are functionally dynamic and shaped by cortical microarchitecture. *eLife*, 9:e61277, November 2020. Publisher: eLife Sciences Publications, Ltd.
- [6] Roxana Zeraati, Tatiana A. Engel, and Anna Levina. A flexible Bayesian framework for unbiased estimation of timescales. *Nature Computational Science*, 2(3):193–204, March 2022.
- [7] Roxana Zeraati, Yan-Liang Shi, Nicholas A Steinmetz, Marc A Gieselmann, Alexander Thiele, Tirin Moore, Anna Levina, and Tatiana A Engel. Intrinsic timescales in the visual cortex change with selective attention and reflect spatial connectivity. *Nature Communications*, 14(1):1858, 2023.
- [8] Alex Graves, Abdel-rahman Mohamed, and Geoffrey Hinton. Speech recognition with deep recurrent neural networks. In *2013 IEEE international conference on acoustics, speech and signal processing*, pages 6645–6649. Ieee, 2013.
- [9] Alex Graves. Generating sequences with recurrent neural networks. *arXiv preprint arXiv:1308.0850*, 2013.
- [10] David Ha and Douglas Eck. A neural representation of sketch drawings. *arXiv preprint arXiv:1704.03477*, 2017.
- [11] Samuel R Bowman, Luke Vilnis, Oriol Vinyals, Andrew M Dai, Rafal Jozefowicz, and Samy Bengio. Generating sentences from a continuous space. *arXiv preprint arXiv:1511.06349*, 2015.
- [12] Junyoung Chung, Caglar Gulcehre, KyungHyun Cho, and Yoshua Bengio. Empirical evaluation of gated recurrent neural networks on sequence modeling. *arXiv preprint arXiv:1412.3555*, 2014.
- [13] José F Torres, Dalil Hadjout, Abderrazak Sebaa, Francisco Martínez-Álvarez, and Alicia Troncoso. Deep learning for time series forecasting: a survey. *Big Data*, 9(1):3–21, 2021.

- [14] Nicolas Boulanger-Lewandowski, Yoshua Bengio, and Pascal Vincent. Modeling temporal dependencies in high-dimensional sequences: Application to polyphonic music generation and transcription. *arXiv preprint arXiv:1206.6392*, 2012.
- [15] Jeffrey L Elman. Finding structure in time. *Cognitive science*, 14(2):179–211, 1990.
- [16] Sepp Hochreiter and Jürgen Schmidhuber. Long short-term memory. *Neural computation*, 9(8):1735–1780, 1997.
- [17] Zachary C Lipton, John Berkowitz, and Charles Elkan. A critical review of recurrent neural networks for sequence learning. *arXiv preprint arXiv:1506.00019*, 2015.
- [18] Yong Yu, Xiaosheng Si, Changhua Hu, and Jianxun Zhang. A review of recurrent neural networks: Lstm cells and network architectures. *Neural computation*, 31(7):1235–1270, 2019.
- [19] Julijana Gjorgjieva, Guillaume Drion, and Eve Marder. Computational implications of biophysical diversity and multiple timescales in neurons and synapses for circuit performance. *Current Opinion in Neurobiology*, 37:44–52, April 2016.
- [20] Renato Duarte, Alexander Seeholzer, Karl Zilles, and Abigail Morrison. Synaptic patterning and the timescales of cortical dynamics. *Current Opinion in Neurobiology*, 43:156–165, April 2017.
- [21] Srdjan Ostojic. Two types of asynchronous activity in networks of excitatory and inhibitory spiking neurons. *Nature Neuroscience*, 17(4):594–600, April 2014.
- [22] Rishidev Chaudhuri, Kenneth Knoblauch, Marie-Alice Gariel, Henry Kennedy, and Xiao-Jing Wang. A Large-Scale Circuit Mechanism for Hierarchical Dynamical Processing in the Primate Cortex. *Neuron*, 88(2):419–431, October 2015.
- [23] Alexander van Meegen and Sacha J. van Albada. Microscopic theory of intrinsic timescales in spiking neural networks. *Physical Review Research*, 3(4):043077, October 2021.
- [24] Ashok Litwin-Kumar and Brent Doiron. Slow dynamics and high variability in balanced cortical networks with clustered connections. *Nature Neuroscience*, 15(11):1498–1505, November 2012. Number: 11 Publisher: Nature Publishing Group.
- [25] Rishidev Chaudhuri, Alberto Bernacchia, and Xiao-Jing Wang. A diversity of localized timescales in network activity. *eLife*, 3, January 2014.
- [26] Yan-Liang Shi, Roxana Zeraati, Anna Levina, and Tatiana A Engel. Spatial and temporal correlations in neural networks with structured connectivity. *Physical Review Research*, 5(1):013005, 2023.
- [27] Nicolas Perez-Nieves, Vincent C. H. Leung, Pier Luigi Dragotti, and Dan F. M. Goodman. Neural heterogeneity promotes robust learning. *Nature Communications*, 12(1):5791, October 2021.
- [28] Corentin Tallec and Yann Ollivier. Can recurrent neural networks warp time? *arXiv preprint arXiv:1804.11188*, 2018.
- [29] Silvan C. Quax, Michele D’Asaro, and Marcel A. J. van Gerven. Adaptive time scales in recurrent neural networks. *Scientific Reports*, 10(1):11360, July 2020. Number: 1 Publisher: Nature Publishing Group.
- [30] Bojian Yin, Federico Corradi, and Sander M. Bohté. Effective and Efficient Computation with Multiple-timescale Spiking Recurrent Neural Networks. In *International Conference on Neuromorphic Systems 2020, ICONS 2020*, pages 1–8, New York, NY, USA, July 2020. Association for Computing Machinery.
- [31] Wei Fang, Zhaofei Yu, Yanqi Chen, Timothee Masquelier, Tiejun Huang, and Yonghong Tian. Incorporating Learnable Membrane Time Constant to Enhance Learning of Spiking Neural Networks, August 2021. arXiv:2007.05785 [cs].

- [32] Jimmy T.H. Smith, Andrew Warrington, and Scott Linderman. Simplified state space layers for sequence modeling. In *The Eleventh International Conference on Learning Representations*, 2023.
- [33] H. Akaike. A new look at the statistical model identification. *IEEE Transactions on Automatic Control*, 19(6):716–723, 1974.
- [34] Dongxian Wu, Shu-Tao Xia, and Yisen Wang. Adversarial weight perturbation helps robust generalization. *Advances in Neural Information Processing Systems*, 33:2958–2969, 2020.
- [35] Sukbin Lim and Mark Goldman. Balanced cortical microcircuitry for maintaining information in working memory. *Nature neuroscience*, 16, 2013.
- [36] Robert Kim and Terrence J. Sejnowski. Strong inhibitory signaling underlies stable temporal dynamics and working memory in spiking neural networks. *Nature Neuroscience*, 24(1):129–139, January 2021.
- [37] Benjamin Cramer, David Stöckel, Markus Kreft, Michael Wibral, Johannes Schemmel, Karlheinz Meier, and Viola Priesemann. Control of criticality and computation in spiking neuromorphic networks with plasticity. *Nature communications*, 11(1):2853, 2020.
- [38] Benjamin Cramer, Markus Kreft, Sebastian Billaudelle, Vitali Karasenko, Aron Leibfried, Eric Müller, Philipp Spilger, Johannes Weis, Johannes Schemmel, Miguel A Muñoz, et al. Autocorrelations from emergent bistability in homeostatic spiking neural networks on neuromorphic hardware. *Physical Review Research*, 5(3):033035, 2023.
- [39] Shivangi Mahto, Vy Ai Vo, Javier S. Turek, and Alexander Huth. Multi-timescale representation learning in {Istm} language models. In *International Conference on Learning Representations*, 2021.
- [40] Jimmy T.H. Smith, Andrew Warrington, and Scott Linderman. Simplified state space layers for sequence modeling. In *The Eleventh International Conference on Learning Representations*, 2023.
- [41] Pengfei Liu, Xipeng Qiu, Xinchu Chen, Shiyu Wu, and Xuan-Jing Huang. Multi-timescale long short-term memory neural network for modelling sentences and documents. In *Proceedings of the 2015 conference on empirical methods in natural language processing*, pages 2326–2335, 2015.
- [42] Martin Gauch, Frederik Kratzert, Daniel Klotz, Grey Nearing, Jimmy Lin, and Sepp Hochreiter. Rainfall–runoff prediction at multiple timescales with a single long short-term memory network. *Hydrology and Earth System Sciences*, 25(4):2045–2062, 2021.
- [43] Jeffrey L Elman. Learning and development in neural networks: The importance of starting small. *Cognition*, 48(1):71–99, 1993.
- [44] Yoshua Bengio, Jérôme Louradour, Ronan Collobert, and Jason Weston. Curriculum learning. In *Proceedings of the 26th Annual International Conference on Machine Learning, ICML ’09*, page 41–48, New York, NY, USA, 2009. Association for Computing Machinery.
- [45] Kai A. Krueger and Peter Dayan. Flexible shaping: How learning in small steps helps. *Cognition*, 110(3):380–394, 2009.
- [46] Daniel R. Kepple, Rainer Engelken, and Kanaka Rajan. Curriculum learning as a tool to uncover learning principles in the brain. In *International Conference on Learning Representations*, 2022.

Appendix

A Different types and location of non-linearity

In order to verify that our results are robust with respect to the type of non-linearity used in the network, we train RNNs using two of the most commonly used non-linearities: ReLU and Tanh. We find that in both cases, the training performance is similar to leaky ReLU, and the development of single-neuron and network-mediated timescales follow the same trajectory as N increases (Fig. S1).

In some implementations of leaky-RNN, the neural self-interaction is linear and located outside of the non-linearity (cf. equ.1)

$$r_i(t) = \left(1 - \frac{1}{\tau_i}\right) \cdot r_i(t-1) + \left[\frac{1}{\tau_i} \cdot \left(\sum_{i \neq j} W_{ij}^R \cdot r_j(t-1) + W_i^I \cdot S(t) + b^R + b^I\right)\right]_{\alpha}. \quad (5)$$

We verify that training RNNs with this implementation gives similar training dynamics and trajectories of τ and τ_{net} with increasing N (Fig. S2), for both curricula. Furthermore, we find that, for large N , ablating neurons with long τ in single-head networks and neurons with short τ in multi-head networks reduces the performance significantly, compatible with the findings in the main text (Fig. S3, cf. Fig. 7).

B Intermediate curricula: multi-head with a sliding window

The two curricula discussed in the main text (single-head and multi-head) represent two extreme cases. In the single-head curriculum, at each step of the curriculum, RNNs are trained to solve a new N without requiring to remember the solution to the previous N s. On the other hand, in the multi-head curriculum, RNNs need to remember the solution to all the previous N s in addition to the new N . Here we test the behavior of curricula that lie in between the two extreme cases.

The intermediate curricula involve the simultaneous training of multiple heads, similar to the multi-head curriculum, but instead of adding new heads at each curriculum step, we train a fixed number of heads and only shift the N s which they are trained for according to a sliding window. We consider the

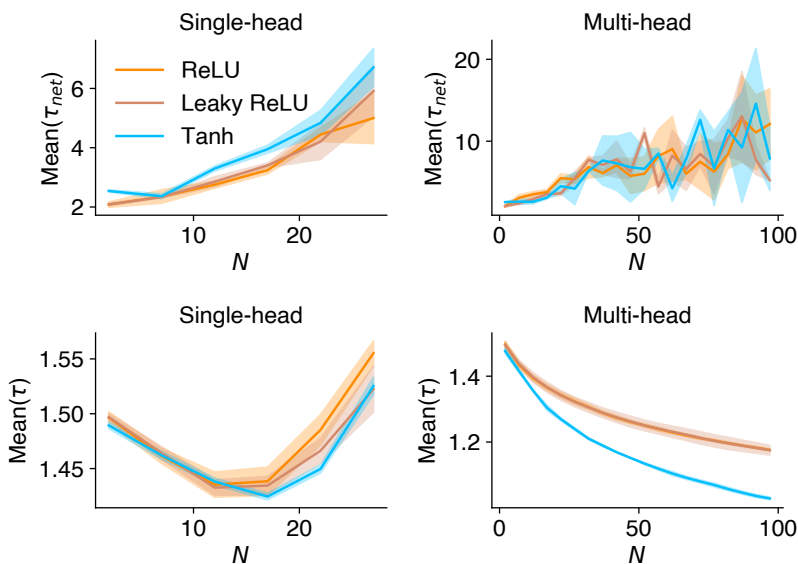


Figure S1: The development of timescales follows similar trajectories when the self-interaction is inside (non-linear τ) or outside (linear τ) the non-linearity (leaky-ReLU). Top: network-mediated timescales, bottom: single-neuron timescales. Shades - \pm STD.

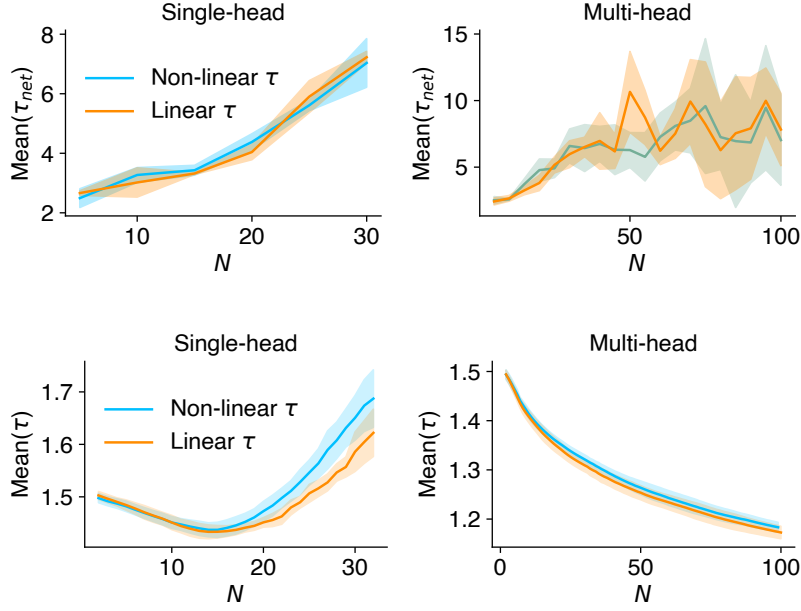


Figure S2: The development of timescales in networks with different non-linearities follows similar trajectories. Top: network-mediated timescales, bottom: single-neuron timescales. Shades - \pm STD.

number of heads to be 10, and start the training for $N \in [2..11]$. In the next steps of the curriculum, we use the already trained network to initialize another network which we train for $N + w$ (e.g., $N \in [2 + w..11 + w]$), where $w \in \{1, 3, 5\}$ indicates the size of the sliding window. For each w , we train 4 different networks (i.e. 4 different initialization). For the following analyses, we trained the networks on the N -parity task.

We find that networks trained with the multi-head-sliding curriculum generally demonstrate an in-between behavior compared with the extreme curricula, but the results also depend on the size of the sliding window. Within 1000 training epochs, the maximal N these networks can solve (with $> 98\%$ accuracy) is in between the maximal N of single- and multi-head curricula, depending on the sliding window. Networks with a larger sliding window can solve a higher maximal N , indicating that a large sliding window not only does not slow down the training but also provides a more efficient curriculum to learn higher N s (Fig. S4a). Moreover, in multi-head-sliding networks, single-neuron (τ) and

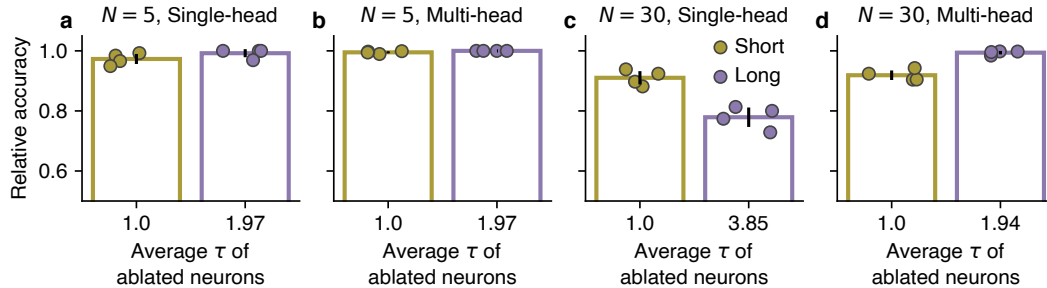


Figure S3: Impact of ablating neurons with distinct timescales on RNNs' performance when neural self-interactions are linear (cf. Fig. 7). **a, b.** Ablating the longest and shortest timescale neurons has minimal effect on network performance when N is small for both curricula. **c, d.** For higher N , ablating long timescale neurons largely decreases the performance of single-head networks, while multi-head networks are more affected by the ablation of short-timescale neurons. Bars - mean, error bars - STD, dots - 4 individual networks.

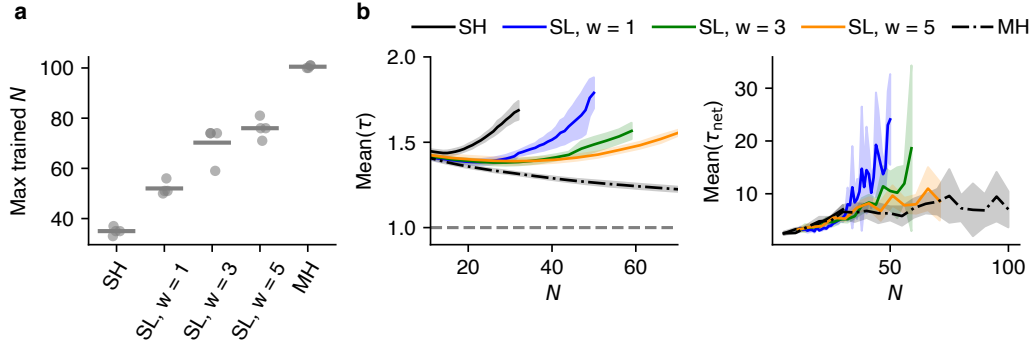


Figure S4: The behavior of networks trained with multi-head-sliding curriculum depends on the size of the sliding window and lies in between extreme curricula. **a.** The maximal trained N (with $> 98\%$ accuracy, within 1000 training epochs) for multi-head-sliding (SL) lies between single-head (SH) and multi-head (MH) networks and increases with the size of sliding window (w). Dots indicate individual networks (4 networks) and the horizontal bars indicate the mean value. **b.** Single-neuron (τ) and network-mediated (τ_{net}) timescales increase with N , but the pace of change reduces as the sliding window grows. Shadings indicate \pm std computed across 4 trained networks.

network-mediated (τ_{net}) timescales have values in between single-head and multi-head curricula (Fig. S4b). However, both τ and τ_{net} grow with N similar to single-head networks, with the pace of growth reducing for larger sliding windows.

Similar to the main text (Fig. 8), we perform the perturbation and re-training analysis on multi-head-sliding networks trained with $w = 5$. The relative accuracy after perturbation of recurrent weights W^R and timescales τ for these networks lies between the two extremes (Fig. S5a, b). However, the re-training analysis suggests that multi-head-sliding networks can be retrained better for higher new N s (Fig. S5c,d). If the network is originally retrained for a small N (e.g., $N = 16$), the re-training relative accuracy is similar between multi-head and sliding networks but is larger than single-head networks. For networks trained for larger N s (e.g., $N = 31$), sliding networks exhibit a superior re-training ability compared to the other two curricula. These results suggest that the curriculum with the sliding window helps multi-head networks to better adjust to new N s.

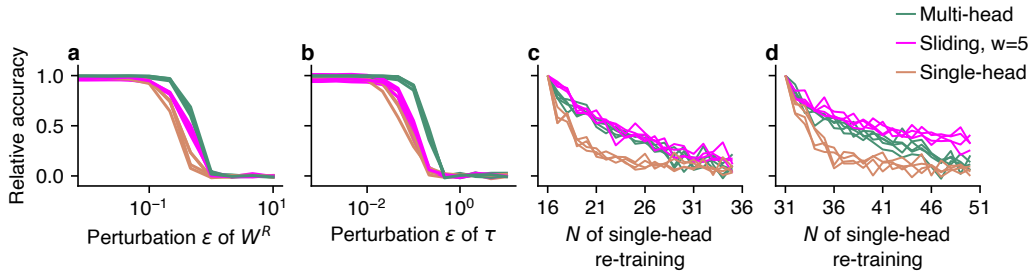


Figure S5: Robustness of networks trained with multi-head-sliding curriculum. **a, b.** Multi-head-sliding networks are more robust than single-head networks but less robust than the multi-head networks against perturbations of recurrent connectivity (a) and trained timescale τ (b). Each line indicates one trained network (4 networks for each curriculum). Shades indicate \pm std computed across 10 trials. **c, d.** Re-training of networks trained with different curricula as a single-head network on new N s (for 20 epochs). Multi-head-sliding networks achieve higher relative accuracy when re-trained for a higher N in comparison to single-head networks. If originally trained for small N s (c, $N = 16$), they have similar re-training accuracy to multi-head networks, but for larger N s (d, $N = 31$) their accuracy suppresses the multi-head networks. Each line indicates the relative accuracy for one network (4 networks for each curriculum).

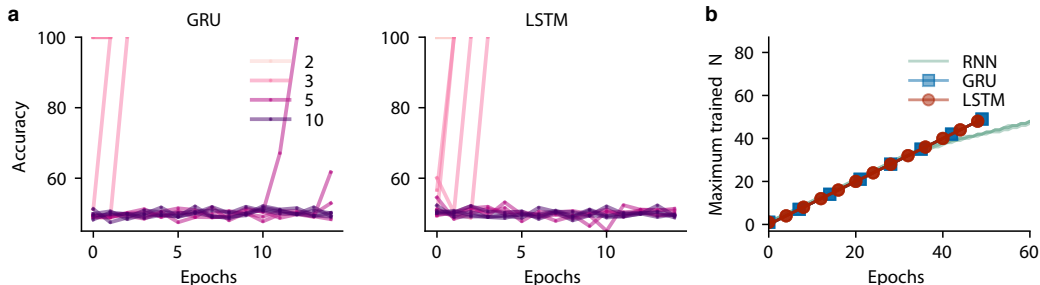


Figure S6: Comparing the impact of curriculum on different recurrent architectures. Two different architectures, GRU and LSTM, are trained on the N -Parity task with and without a curriculum. We observe that the GRU and LSTM both exhibit instability when training without a curriculum (a), but are comparable to the RNNs with the multi-head curriculum (b).

C Single- and multi-head curricula for training GRU and LSTM

The results presented in the main text were generated using a modified version of a vanilla RNN (leaky-RNN) with an explicit definition of the timescale parameter τ . To test whether the difficulties in training for long memory tasks without curriculum would carry over to recurrent networks that were specifically designed for long memory tasks, we train two other architectures, an LSTM (long short-term memory) and a GRU (gated recurrent unit) on the N -parity task for increasing N , with and without a curriculum. Both the GRU and LSTM have similar network sizes to the RNN with 500 neurons, though they differ in their activation functions (the RNN used a single leakyReLU whereas the GRU/LSTMs have both sigmoids and tanhs for different gates). Furthermore, in contrast with the RNNs, an Adam optimizer is used with learning rate $lr = 10^{-3}$ and the input signals to the models take values $\in \{-1, 1\}$ (to have a zero-mean input signal).

We find that for both architectures, training the networks without a curriculum is extremely slow for large N and relatively unstable for small N and probably requires strict hyper-parameter tuning (Fig. S6a). Without additional hyper-parameter tuning, introducing the multi-head curriculum speeds up the training significantly, and both architectures can easily learn the N -parity task with large N similar to the leaky-RNN (Fig. S6b). Moreover, similar to RNNs, the multi-head curriculum has a higher training speed than the single-head curriculum (Fig. S7). Our results indicate that GRUs and LSTMs are subject to similar training dynamics as RNNs used in the main text and the multi-head curriculum is an optimal curriculum regardless of the RNN architecture. The advantage of using the leaky-RNN architecture is that its parameters are easier to interpret and it allows us to better study the mechanisms underlying each curriculum by explicitly studying the role of timescales.

D Emergence of curriculum during multi-head training

In the multi-head curriculum, the difficulty of the task increases gradually; a new head with a larger N is added at each step of the curriculum. In the main text, we discussed that networks trained with

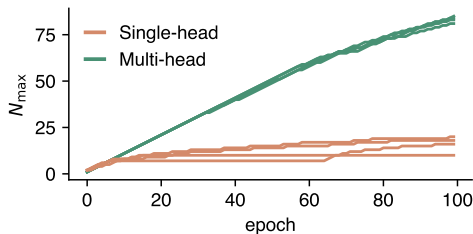


Figure S7: Comparison of single- and multi-head curricula for training LSTMs on N -parity task. Networks trained with the multi-head curriculum can reach a higher N faster than networks trained with the single-head curriculum.

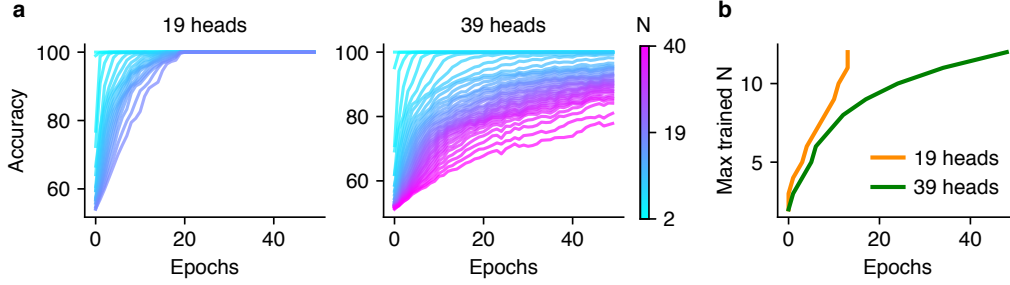


Figure S8: Emergence of curriculum during multi-head training. **a.** In the absence of an explicit curriculum, multi-head networks solve smaller N s before solving the large N s. The color bar indicates the range of N s. **b.** The speed of training reduces with the increasing number of heads. The network with 19 heads needs fewer epochs to solve the same N (i.e. reaching 98% accuracy) than the network with 39 heads.

such a curriculum generally train well up to large N s. Here we ask whether this optimal curriculum can emerge by itself if we train a network with multiple heads, but without any predefined curricula. For this analysis, we train RNNs with 19 ($N \in [2..20]$) and 39 heads ($N \in [2..40]$) to solve all the available N s simultaneously.

We find that despite the absence of an explicit curriculum, these networks learn the task by generating an internal multi-head curriculum. While all the heads contribute equally to the loss, heads with a smaller N reach the higher accuracy faster (Fig. S8a). However, the speed of training strongly depends on the total number of heads in each network. For the same N , the network with 19 heads reaches the 98% accuracy faster than the network with 39 heads (Fig. S8b), but both networks have a slower training speed when compared to the multi-head curriculum. These results suggest that the multi-head curriculum is an optimal curriculum that can arise naturally during multi-head training and can increase the training speed when applied explicitly.

E Time-rescaling of input

In our tasks, input contains two timescales: the timescale of updating inputs k (i.e., the number of time steps that a single digit of input is presented to the network), and the timescale of the task's memory N . k acts as a time-rescaling parameter and defines one unit of time for the task performance. In the analysis of the main text, we considered $k = 1$. Here, we train the RNNs with different values of $k \in \{2, 3, 5, 10\}$ and test whether similar trajectories of τ with N can be observed.

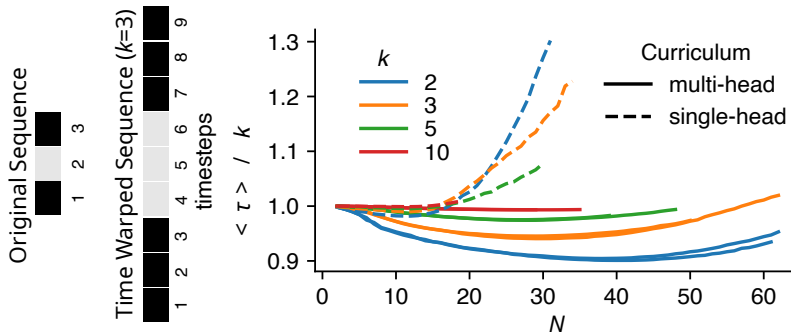


Figure S9: Training with time-rescaled inputs. Each digit of input is presented to RNN over k consecutive time steps. Single-neuron timescales (τ s) rescaled by k remain roughly constant in multi-head networks and increase with N in single-head networks (cf. Fig. 4b).

We find that similar to the case with $k = 1$, single-head networks trained with $k > 1$ increase their τ with N , while multi-head networks try to keep τ close to k (Fig. S9). Moreover, tasks with $k > 1$ are generally more difficult to solve, since the input needs to be tracked over $N \cdot k$ time steps. Hence, as k grows, RNNs would reach smaller N within the same number of training epochs. The changes in values of τ after rescaling with k might be due to non-linear interactions in the network arising from the combination of different N and k .

F Ablation details

To test whether neurons with fast or slow timescales (τ) are necessary for computations in the trained RNNs we perform the ablation analysis. For this analysis, we compute the relative accuracy of the model (Eq. 4 in the main text) after removing a single neuron. We ablate neuron i by setting all incoming and outgoing associated weights to zero

$$\begin{aligned} W_{ij}^R &= 0 & \forall j \\ W_{ji}^R &= 0 & \forall j \\ W_i^O &= 0 \\ W_i^I &= 0 \end{aligned} \tag{6}$$

Here W_{ij}^R refers to recurrent weights, W_i^O to input weights and W_i^I to readout weights. To measure the relative accuracy, we simulate the RNN forward using random binary inputs for 1000 timesteps after 100 timesteps of a burn-in period (to reach the stationary state). Then, we evaluate the accuracy of the network at each timestep. We repeat this procedure over 10 trials and compute the average and standard deviation of the relative accuracies across trials.

G Additional supplementary figures

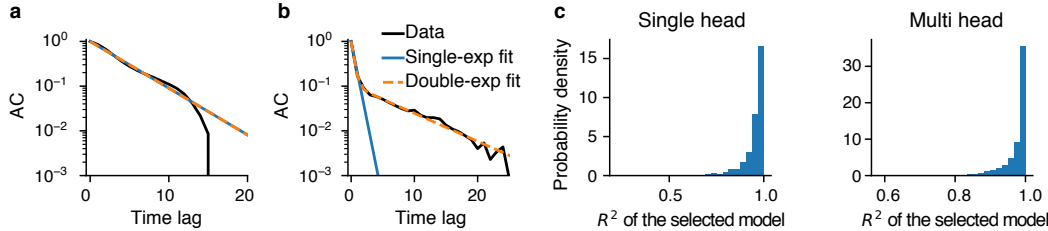


Figure S10: Autocorrelations of neurons are well captured with single- or double-exponential fits. **a, b.** Fitting double and single exponential functions to the autocorrelation (AC) of example (a) single-timescale ($\tau_{\text{net}} = \tau$) and (b) double timescale ($\tau_{\text{net}} > \tau$) neurons. **c.** Values of coefficient of determination R^2 estimated for all selected fits using AIC are close to 1, indicating a good fit.

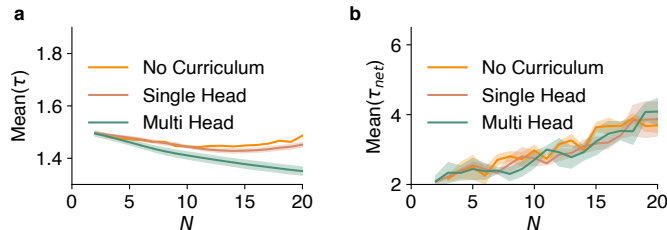


Figure S11: Networks trained without curriculum have similar single-neuron **(a)** and network-mediated **(b)** timescales to networks trained with the single-head curriculum in the range of N that the no-curriculum-trained networks can learn.